

Heavy metal glasses and transparent glass-ceramics: preparation, local structure and optical properties

JOANNA PISARSKA^{1*}, TOMASZ GORYCZKA², LIDIA ŻUR¹, WOJCIECH A. PISARSKI¹

¹University of Silesia, Institute of Chemistry, Szkolna 9, 40-007 Katowice, Poland

²University of Silesia, Institute of Materials Science, Bankowa 12, 40-007 Katowice, Poland

*Corresponding author: joanna.pisarska@us.edu.pl

Heavy metal oxide and oxyfluoride lead silicate glasses doped with rare-earth ions were prepared. Next, they were heat treated in order to obtain transparent glass-ceramics. The rare-earths as optically active ions were limited to trivalent Eu^{3+} and Dy^{3+} . Correlation between the local structure and the luminescence properties of Eu^{3+} and Dy^{3+} ions in the studied glass and glass-ceramic systems was examined using X-ray diffraction, FT-IR and optical measurements. Especially, the ratio of integrated emission intensity of the ${}^5D_0\text{--}{}^7F_2$ transition to that of the ${}^5D_0\text{--}{}^7F_1$ transition of Eu^{3+} , defined as the luminescence intensity ratio R (Eu^{3+}) as well as the ratio of integrated emission intensity of the ${}^4F_{9/2}\text{--}{}^6H_{13/2}$ transition to that of the ${}^4F_{9/2}\text{--}{}^6H_{15/2}$ transition of Dy^{3+} , defined as the luminescence intensity ratio Y/B (Dy^{3+}), have been analyzed in details. Their values are reduced due to part incorporation of rare-earth ions into cubic $\beta\text{-PbF}_2$ crystalline phase. The excitation and luminescence spectra of rare-earth ions in glass samples before and after heat treatment are presented and discussed in relation to potential application in optoelectronics.

Keywords: heavy metal glasses, glass-ceramics, heat treatment, rare-earth ions, luminescence.

1. Introduction

Rare-earth doped lead silicate glasses and glass fibers belong to the wide family of heavy metal oxide systems, which are promising for near-infrared luminescence and upconversion applications [1–4]. The presence of a lead fluoride component in lead silicate glass improves spectroscopic properties of rare-earth ions and gives possibility to obtain fluoride nanocrystals dispersed into a base oxide matrix [5]. Heat treatment process [6] or diode-laser irradiation [7] of precursor lead silicate glasses is an efficient way to fabricate transparent glass-ceramics containing cubic PbF_2 crystals, usually in the nanometric scale.

The incorporation of Eu^{3+} and Dy^{3+} ions to heavy metal glass materials is promising for efficient red and yellow/blue luminescence. Moreover, trivalent europium and dysprosium ions in many glass systems play an important role as a spectroscopic probe [8]. The ratio of integrated emission intensity of the ${}^5D_0\text{--}{}^7F_2$ transition to that

of the ${}^5D_0-{}^7F_1$ transition of Eu^{3+} , defined as the luminescence intensity ratio R (Eu^{3+}) as well as the ratio of integrated emission intensity of the ${}^4F_{9/2}-{}^6H_{13/2}$ transition to that of the ${}^4F_{9/2}-{}^6H_{15/2}$ transition of Dy^{3+} , defined as the luminescence intensity ratio Y/B (Dy^{3+}), can be modulated by varying the glass host composition, activator concentration and heat treatment. The latter process leads to transformation from glasses to transparent glass-ceramics (TGC), as mentioned above. The spectroscopic consequence of this transformation is the narrowing of spectral lines of rare-earth ions and the change of luminescence intensity ratios R (Eu^{3+}) and Y/B (Dy^{3+}). This behaviour can be explained by structural changes in the environment around rare-earth ions, giving important contribution to the luminescence intensities associated with appropriate transitions of Eu^{3+} and Dy^{3+} .

Presented research has been focused on novel $\text{PbF}_2\text{-PbO-SiO}_2\text{-Ga}_2\text{O}_3\text{-Ln}_2\text{O}_3$ glasses (where Ln denotes Eu or Dy), which were thermally treated in order to fabricate transparent glass-ceramic systems. The local structure was confirmed by XRD and FT-IR spectroscopy. Next, the glass samples before and after heat treatment were examined using luminescence spectroscopy.

2. Experimental techniques

The X-ray diffraction was carried out using INEL diffractometer with $\text{Cu K}\alpha$ radiation. The FT-IR spectra were performed by Bruker spectrometer using standard KBr disc techniques. Excitation and luminescence spectra were performed using Jobin Yvon Fluoromax 4 spectrophotometer. The spectral resolution was equal to 0.1 nm. All spectral measurements were carried out at room temperature.

3. Results and discussion

3.1. Glass preparation and heat treatment

Glass samples with composition (mol%): $9\text{PbF}_2\text{-}36\text{PbO-}45\text{SiO}_2\text{-}9.5\text{Ga}_2\text{O}_3\text{-}0.5\text{Ln}_2\text{O}_3$ were synthesized, where Ln denotes Eu or Dy. Anhydrous oxides and lead fluoride (99.99% purity, Aldrich) were used as starting materials. Glasses were melted at 1100 °C for 0.5 h in Pt crucibles, then poured into preheated copper moulds and annealed below glass transition temperature. After this procedure, the samples were slowly cooled to room temperature. Transparent glassy plates were obtained in thickness of about 2 mm.

In order to prepare transparent glass-ceramics, the precursor oxyfluoride lead silicate glasses were annealed at 450 °C for 5–15 h. The heat treatment conditions were experimentally determined based on glass transition temperature T_g obtained from DSC curves and several tests of controlled crystallization of precursor glasses [9].

3.2. Local glass structure

The local glass structure was examined using X-ray diffraction and FT-IR spectroscopy. Figure 1 presents typical FT-IR spectrum for the studied system.

The near-infrared bands for lead silicate glass were assigned based on literature data [10]. The band in the $460\text{--}520\text{ cm}^{-1}$ frequency region corresponds to Pb–O stretching vibrations of the $[\text{PbO}_4]$ structural units along with the deformation modes of the Si–O glass network. The FT-IR bands due to the asymmetric stretching vibrational modes of silica tetrahedra are located in the $600\text{--}1150\text{ cm}^{-1}$ frequency region. They are attributed to Q^n ($n = 0\text{--}3$) species and the main FT-IR band originates mainly from Q^3 species [10].

In order to obtain information on the crystallizing phases during heat treatment process, the X-ray diffraction was performed. Figure 2 shows X-ray diffraction patterns for glass samples before and after heat treatment. For precursor glasses, the XRD pattern displays two characteristic broad bands corresponding to the fully amorphous phases and does not show any strong diffraction lines due to the crystalline phases.

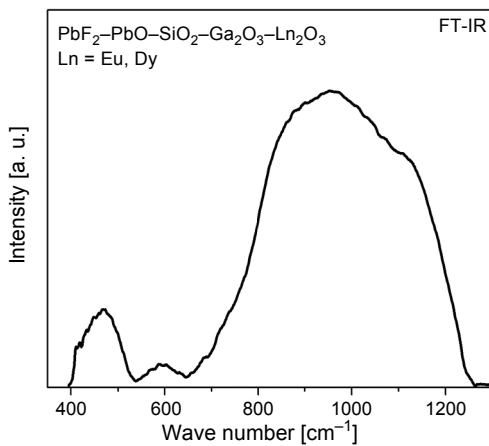


Fig. 1. FT-IR spectrum for the $\text{PbF}_2\text{--PbO--SiO}_2\text{--Ga}_2\text{O}_3\text{--Ln}_2\text{O}_3$ glass (Ln = Eu or Dy).

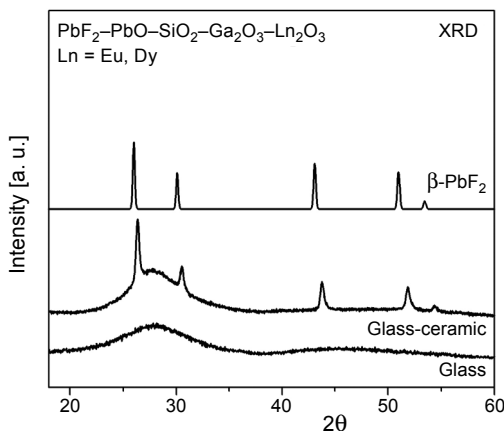


Fig. 2. X-ray diffraction pattern for the $\text{PbF}_2\text{--PbO--SiO}_2\text{--Ga}_2\text{O}_3\text{--Ln}_2\text{O}_3$ glass (Ln = Eu or Dy) before and after heat treatment.

During controlled crystallization of precursor glasses, several narrowed diffraction lines were successfully formed. Crystalline peaks are due to the cubic β -PbF₂ phase (PDF-2 card no. P060251).

3.3. Optical properties

Figure 3 presents luminescence spectra for Eu³⁺ and Dy³⁺ ions in glass samples before and after heat treatment. Several luminescence bands due to the $^5D_0-^7F_J$ ($J = 0, 1, 2, 3, 4$) transitions of Eu³⁺ ions can be observed. Two of them presented in Fig. 3, the $^5D_0-^7F_1$ magnetic-dipole transition located at 590 nm (orange line) and $^5D_0-^7F_2$ electric-dipole transition near 610 nm (red line), are the main luminescence lines of Eu³⁺. For Dy³⁺-doped system, we observe three luminescence bands at 480 nm (blue line), 573 nm (yellow line) and 662 nm (red line) due to the $^4F_{9/2}-^6H_{J/2}$ ($J = 15, 13, 11$) transitions of Dy³⁺. The main intense blue and yellow bands are due to the $^4F_{9/2}-^6H_{15/2}$ and $^4F_{9/2}-^6H_{13/2}$ electric-dipole transitions of Dy³⁺ ions, respectively. It is clearly visible from the spectra, that the intensities of the main luminescence lines of Eu³⁺ and Dy³⁺ strongly depend on the surrounding rare-earth ions, which were drastically changed after heat treatment process.

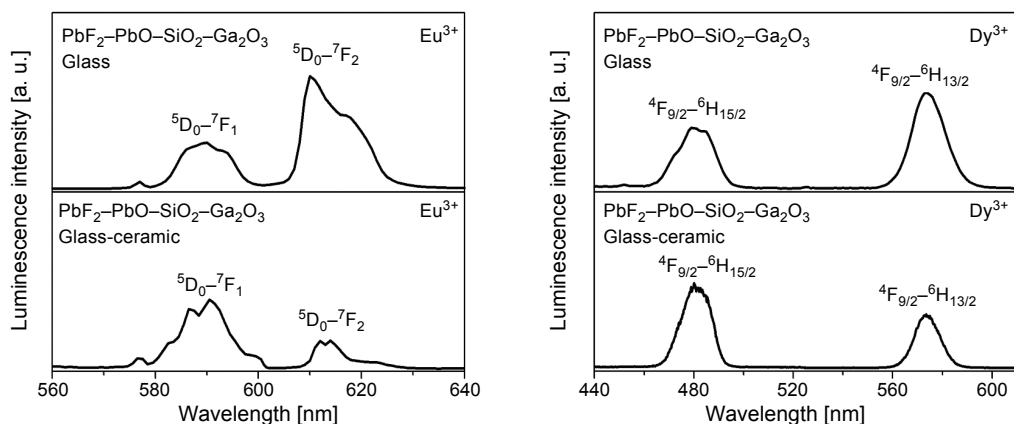


Fig. 3. Luminescence spectra for Eu³⁺ (left) and Dy³⁺ (right) ions in the heavy metal oxyfluoride lead silicate glass systems before and after heat treatment.

The luminescence intensity ratio R is relative to the strength of covalent/ionic bonding between the Eu³⁺ ion and the surrounding ligands. The $^5D_0-^7F_1$ transition is a magnetic-dipole transition, which is independent of the local symmetry. Therefore, the intensity ratio of the $^5D_0-^7F_2$ transition to the $^5D_0-^7F_1$ transition is a spectroscopic key to estimate the deviation from the site symmetries of the Eu³⁺ ions. This ratio is a sensitive function of covalency and asymmetry around the Eu³⁺ ions. Small R value is usually attributed to higher local symmetry for Eu³⁺ ions. The increase in R value

is due to increasing asymmetry and degree of covalency between europium and oxygen ions. The intensity of emission due to ${}^4F_{9/2}-{}^6H_{13/2}$ transition is strongly influenced by the environment, in comparison to less sensitive ${}^4F_{9/2}-{}^6H_{15/2}$ transition of Dy^{3+} ions. It results in different luminescence intensity ratios Y/B of Dy^{3+} . The higher values of Y/B indicate the higher degree of covalency between dysprosium and oxygen ions.

From accumulated experience it is known that luminescence intensity ratios R of Eu^{3+} and Y/B of Dy^{3+} are quite different for glass samples before and after heat treatment. The reduced values of R (Eu^{3+}) and Y/B (Dy^{3+}) for our heat-treated glass samples were determined [9]. During the heat treatment of precursor $\text{PbF}_2\text{-PbO-SiO}_2\text{-Ga}_2\text{O}_3\text{-Ln}_2\text{O}_3$ ($\text{Ln} = \text{Eu}$ or Dy) glasses, transparent glass-ceramic systems containing cubic $\beta\text{-PbF}_2$ phase were successfully prepared. The site environment of the optically active ions was changed and ionic bonding character increased due to the presence of $\text{Ln}^{3+}\text{-F}^-$ bonds, because part of Ln^{3+} ions ($\text{Ln} = \text{Eu}, \text{Dy}$) is incorporated into PbF_2 crystalline phase. It results in the change in relative intensities of luminescence bands associated with the ${}^5D_0-{}^7F_2$ and ${}^5D_0-{}^7F_1$ transitions of Eu^{3+} as well as the ${}^4F_{9/2}-{}^6H_{15/2}$ and ${}^4F_{9/2}-{}^6H_{13/2}$ transitions of Dy^{3+} . The reduction of both R (Eu^{3+}) and Y/B (Dy^{3+}) parameters in TGC system is attributed to the PbF_2 crystalline environment of Ln^{3+} ions. These spectroscopic changes were also detected for Eu^{3+} [11–13] and Dy^{3+} [14–16] ions in similar mixed oxyfluoride glasses after heat treatment. The luminescence lifetime for the excited state of rare-earth ions is the second important spectroscopic parameter, which informs us about optical changes related to structural transformation from glass to glass-ceramic. The change of rare-earth surroundings is the consequence of this transformation. The value of luminescence lifetime should be considerably enhanced, when part of rare-earth ions is incorporated into fluoride crystalline PbF_2 phase. These phenomena will be examined and discussed in a separate work.

4. Conclusions

Selected oxyfluoride lead silicate glasses containing Eu^{3+} and Dy^{3+} ions were heat treated in order to obtain transparent glass-ceramics. Luminescence spectra for Eu^{3+} and Dy^{3+} ions in glass samples before and after heat treatment were registered. The relative band intensities due to ${}^5D_0-{}^7F_2$ and ${}^5D_0-{}^7F_1$ transitions of Eu^{3+} as well as the ${}^4F_{9/2}-{}^6H_{15/2}$ and ${}^4F_{9/2}-{}^6H_{13/2}$ transitions of Dy^{3+} , referred to as luminescence intensity ratios R (Eu^{3+}) and Y/B (Dy^{3+}), have been analyzed in details. A spectroscopic consequence of the transformation from glasses to transparent glass-ceramics is reduction of R (Eu^{3+}) and Y/B (Dy^{3+}) values, which clearly indicates that Ln^{3+} ions are partially incorporated into $\beta\text{-PbF}_2$ crystalline phase.

Acknowledgements – The Ministry of Science and Higher Education (Poland) supported this work under grant No. N N204 313937.

References

- [1] BETTINELLI M., SPEGHINI A., BRIK M.G., *Spectroscopic studies of emission and absorption properties of 38PbO–62SiO₂:Nd³⁺ glass*, *Optical Materials* **32**(12), 2010, pp. 1592–1596.
- [2] CAPOBIANCO J.A., PREVOST G., PROULX P.P., KABRO P., BETTINELLI M., *Upconversion properties of Er³⁺ doped lead silicate glasses*, *Optical Materials* **6**(3), 1996, pp. 175–184.
- [3] KARMAKAR B., DWIVEDI R.N., *FT-IRRS, UV–Vis–NIR absorption and green upconversion in Er³⁺ doped lead silicate glass*, *Journal of Non-Crystalline Solids* **342**(1–3), 2004, pp. 132–139.
- [4] WANG J., REEKIE L., BROCKLESBY W.S., CHOW Y.T., PAYNE D.N., *Fabrication, spectroscopy and laser performance of Nd³⁺-doped lead-silicate glass fibers*, *Journal of Non-Crystalline Solids* **180**(2–3), 1995, pp. 207–216.
- [5] FANQING ZENG, GUOZHONG REN, XIANNIAN QIU, QIBIN YANG, JINGWU CHEN, *The effect of PbF₂ content on the microstructure and upconversion luminescence of Er³⁺-doped SiO₂–PbF₂–PbO glass ceramics*, *Journal of Non-Crystalline Solids* **354**(29), 2008, pp. 3428–3432.
- [6] TIKHOMIROV V.K., FURNESS D., SEDDON A.B., REANEY I.M., BEGGIORA M., FERRARI M., MONTAGNA M., ROLLI R., *Fabrication and characterization of nanoscale, Er³⁺-doped, ultratransparent oxy-fluoride glass ceramics*, *Applied Physics Letters* **81**(11), 2002, pp. 1937–1939.
- [7] GONZALEZ-PEREZ S., MARTIN I.R., JAQUE D., HARO-GONZALEZ P., CAPUJ N., *Control of the local devitrification on oxyfluoride glass doped with Er³⁺ ions under diode laser irradiation*, *Journal of Applied Physics* **108**(10), 2010, article 103103.
- [8] PISARSKI W.A., PISARSKA J., DOMINIAK-DZIK G., RYBA-ROMANOWSKI W., *Transition metal (Cr³⁺) and rare earth ions (Eu³⁺, Dy³⁺) used as a spectroscopic probe in compositional-dependent lead borate glasses*, *Journal of Alloys and Compounds* **484**(1–2), 2009 pp. 45–49.
- [9] PISARSKA J., ŻUR L., PISARSKI W.A., *Transparent glass-ceramics containing Eu³⁺ and Dy³⁺ ions for visible optoelectronics*, *Proceedings of SPIE* **8010**, 2011, article 80100N.
- [10] FELLER S., LODDEN G., RILEY A., EDWARDS T., CROSKREY J., SCHUE A., LISS D., STENTZ D., BLAIR S., KELLEY M., SMITH G., SINGLETON S., AFFATIGATO M., HOLLAND D., SMITH M.E., KAMITSOS E.I., VARSAMIS C.P.E., IOANNOU E., *A multispectroscopic structural study of lead silicate glasses over an extended range of compositions*, *Journal of Non-Crystalline Solids* **356**(6–8), 2010, pp. 304–313.
- [11] DRIESEN K., TIKHOMIROV V.K., GORLLER-WALRAND C., *Eu³⁺ as a probe for rare-earth dopant site structure in nano-glass-ceramics*, *Journal of Applied Physics* **102**(2), 2007, article 024312.
- [12] DALIANG ZHAO, XVSHENG QIAO, XIANPING FAN, MINQUAN WANG, *Local vibration around rare earth ions in SiO₂–PbF₂ glass and glass ceramics using Eu³⁺ probe*, *Physica B* **395**(1–2), 2007, pp. 10–15.
- [13] BUENO L.A., GOUVEIA-NETO A.S., DA COSTA E.B., MESSADDEQ Y., RIBEIRO S.J.L., *Structural and spectroscopic study of oxyfluoride glasses and glass-ceramics using europium ion as a structural probe*, *Journal of Physics: Condensed Matter* **20**(14), 2008, article 145201.
- [14] BABU P., KYOUNG HYUK JANG, EUN SIK KIM, LIANG SHI, HYO JIN SEO, RIVERA-LOPEZ F., RODRIGUEZ-MENDOZA U.R., LAVIN V., VIJAYA R., JAYASANKAR C.K., RAMA MOORTHY L., *Spectral investigations on Dy³⁺-doped transparent oxyfluoride glasses and nanocrystalline glass ceramics*, *Journal of Applied Physics* **105**(1), 2009, article 013516.
- [15] BABU P., KYOUNG HYUK JANG, EUN SIK KIM, LIANG SHI, VIJAYA R., LAVIN V., JAYASANKAR C.K., HYO JIN SEO, *Optical properties and energy transfer of Dy³⁺-doped transparent oxyfluoride glasses and glass-ceramics*, *Journal of Non-Crystalline Solids* **356**(4–5), 2010, pp. 236–243.
- [16] PISARSKA J., ŻUR L., PISARSKI W.A., *Optical spectroscopy of Dy³⁺ ions in heavy metal lead-based glasses and glass-ceramics*, *Journal of Molecular Structure* **993**(1–3), 2011, pp. 160–166.

*Received August 23, 2011
in revised form December 23, 2011*